• Supplementary File •

Spintronic-metasurface terahertz emitters with magnetic-field manipulated polarizations

Qing YANG¹, Yan HUANG¹, Houyi CHENG^{1,2}, Jie ZHANG¹, Fan ZHANG^{1,2}, Yong XU^{1,3}, Lianggong WEN^{1,4}, Weisheng ZHAO^{1,2,3,4} & Tianxiao Nie^{1,2,3,4}*

¹MIIT Key Laboratory of Spintronics, School of Integrated Circuit Science and Engineering, Beihang University, Beijing 100191, China
²Hefei Innovation Research Institute, Beihang University, Hefei 230012, China
³National Key Lab of Spintronics, Institute of International Innovation, Beihang University, Yuhang District, Hangzhou, 311115, China
⁴Qingdao Innovation Research Institute, Beihang University, Qingdao 266000, China

Appendix A The details of measurement setup

The terahertz time domain spectroscopy (THz-TDS) system used in our experiment is driven by a commercial amplified Ti: sapphire laser source delivering a central wavelength of 800 nm, a pulse duration of 35 fs and a repetition rate of 1 KHz. The non-uniform magnetic field is confined to the xy plane without any component in the z-direction, which allows terahertz waves to propagate along the z-axis. In the far field, the detected terahertz waves are the effect of interactions occurring at various points. Consequently, we consider only the polarization of the terahertz waves as they exist within the xy plane. Here, we use two terahertz polarizers (P1 and P2) and electro-optic sampling (EOS) methods to detect chiral terahertz waves. The measurement setup is illustrated in the figure below. The laser pulses are divided into two beams where one beam with 90% energy named excitation pulse and the other with 10% energy called probe pulse. The former with 8 mm spot diameter is used to pump the patterned spintronic terahertz emitters for terahertz waves generation, and the latter is applied to probe the generated terahertz waves. The terahertz polarizer P1 is mounted on the convergence position of vertical axis paraboloid mirror and P2 is installed in the middle of the third and the last. To guarantee the accuracy of terahertz polarization measurement, the grid of P2 keeps consistent with the orientation of external magnetic field and P1 is used to be adjusted to $\pm 45^{\circ}$ with respect to P2 called as E_v and E_u . The component in the x direction E_x $= E_v + E_u$, while the component in the y-direction is $E_u = E_v - E_u$. The THz waves are combined by a pellicle, the probe pulse is focused on a 2 mm thick ZnTe crystal, through a quarter-wave plate, a Wollaston prism, and collected by a pair of photodiodes.

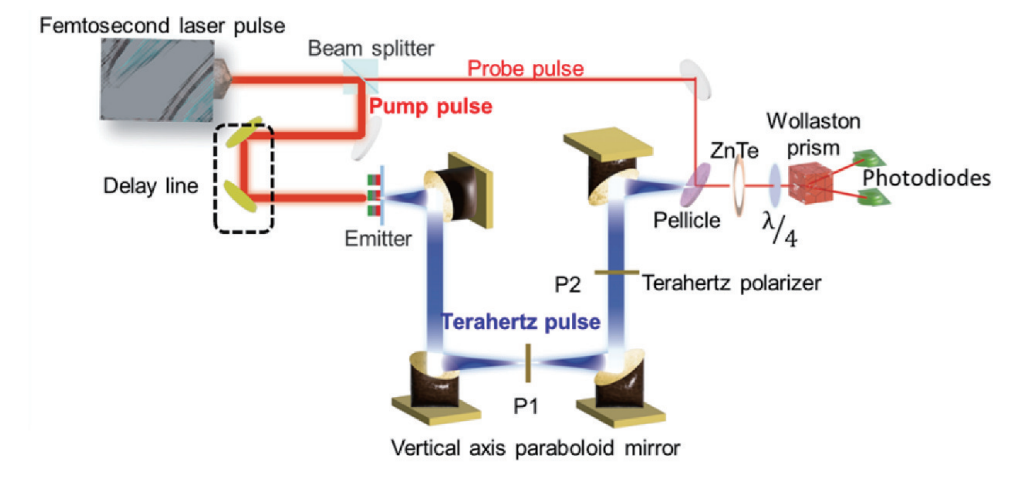


Figure A1 The measurement equipment of the polarization-resolved terahertz time domain spectroscopy system. Two terahertz polarizers (P1 and P2) are crucial to detect terahertz polarization waves.

 $[\]hbox{* Corresponding author (email: nietianxiao@buaa.edu.cn)}\\$

We used commercial neodymium magnets to generate various magnetic field distributions. By using static magnets of different thicknesses ranging from 1 mm to 10 mm, the magnetic field strength in the center can vary from 20 mT to 100 mT when the magnets attract each other. The distance between the two magnets is approximately 37 mm.

Non-uniform magnetic fields are obtained when the two south (or north) poles of magnets of the same thickness face each other. The magnetic field strength in the center, measured by a magnetometer, can increase from 2 mT to 40 mT, depending on the thickness and number of static magnets used.

To ensure the accuracy of the experimental results, we positioned the emitter at the same location as the magnetometer.

Appendix B The polarization modulation results of relevant analysis

According to the inverse spin Hall effect (ISHE), j_c is expressed by $j_c = \gamma j_s \times M/|M|$, where γ is the magnitude of spin Hall angles, is is the injected spin current, and M is the magnetization. It is evident that j_c is always perpendicular to M. Therefore, the distribution and direction of magnetic field play a decisive role in terahertz emission. When femtosecond laser pulses illuminate on the unevenly magnetized stripe emitter, it will generate two spin-converted in-plane transverse ultrafast charge currents j_{cx} and j_{cy} with their predominant flowing directions perpendicular to the corresponding dominated magnetic fields M_x and M_y . Upon charges generated, electrons accumulate at the edge of stripe in the W and Pt layer, while an equal number of positive charges gather at the other side accordingly in accordance with the law of charge conservation, resulting in the built-in electric field E_i that is opposite to the gap-electric field E_s . Charges on both edges of the stripe are attracted to each other by E_i and E_s , which helps to confine them to the boundaries. When the ratio l/w is greater than l/d, E_i is stronger than E_s , and charges will flow in the opposite direction to j_c , forming the backflow j_i . To establish a clearer connection between j_c and j_i , we decompose j_{cx} and j_{cy} into two components: j_{cv} , which is perpendicular to the direction of stripe arrangement, and j_{cp} , which is parallel to the direction of stripe arrangement. Correspondingly, j_i is divided into j_{iv} and j_{ip} . Note that the relevant component of j_i come from the accumulating charges, so j_{iv} and j_{ip} cannot be calculated directly by vector decomposition. We define j_{iv} and j_{ip} at the initial moment as j_a and j_b , respectively. During the rotating process, the back flow and charges distribution are deeply affected by the azimuth angle, so each current can be represented by j_c , j_a , j_b and corresponding azimuth angles. The analysis process is illustrated in Figure B1(a) and (b). As for $0^{\circ} < \varphi < 90^{\circ}$, each current meet:

$$j_{cv} = j_{cx} cos\varphi + j_{cy} sin\varphi, \tag{B1}$$

$$j_{cp} = j_{cx} \sin\varphi - j_{cy} \cos\varphi, \tag{B2}$$

$$j_{iv} = j_a cos\varphi - j_b sin\varphi, \tag{B3}$$

$$j_{ip} = -j_a sin\varphi + j_b cos\varphi, \tag{B4}$$

As for $90^{\circ} < \varphi < 180^{\circ}$, each current meet:

$$j_{cv} = j_{cx} \cos \varphi - j_{cy} \sin \varphi, \tag{B5}$$

$$j_{cp} = j_{cx} \sin\varphi + j_{cy} \cos\varphi, \tag{B6}$$

$$j_{iv} = j_a \cos\varphi - j_b \sin\varphi, \tag{B7}$$

$$j_{ip} = j_a sin\varphi - j_b cos\varphi, \tag{B8}$$

Owing to detection terminal of THz-TDS towards x and y directions, each current along sides should be divided into x and y directions for polarization analysis.

During rotating from 0° to 90°, current in the x direction is:

$$j_x = j_{cx} \sin\varphi - j_{a} \cos 2\varphi, \tag{B9}$$

During rotating from 90° to 180°,

$$j_x = j_{cx} \sin \varphi - j_a \cos 2\varphi, \tag{B10}$$

$$j_y = j_b - j_a \sin 2\varphi + j_{cy}, \tag{B11}$$

when $\varphi > 90^{\circ}$,

$$j_y = -j_b + j_a \sin 2\varphi + j_{cy}, \tag{B12}$$

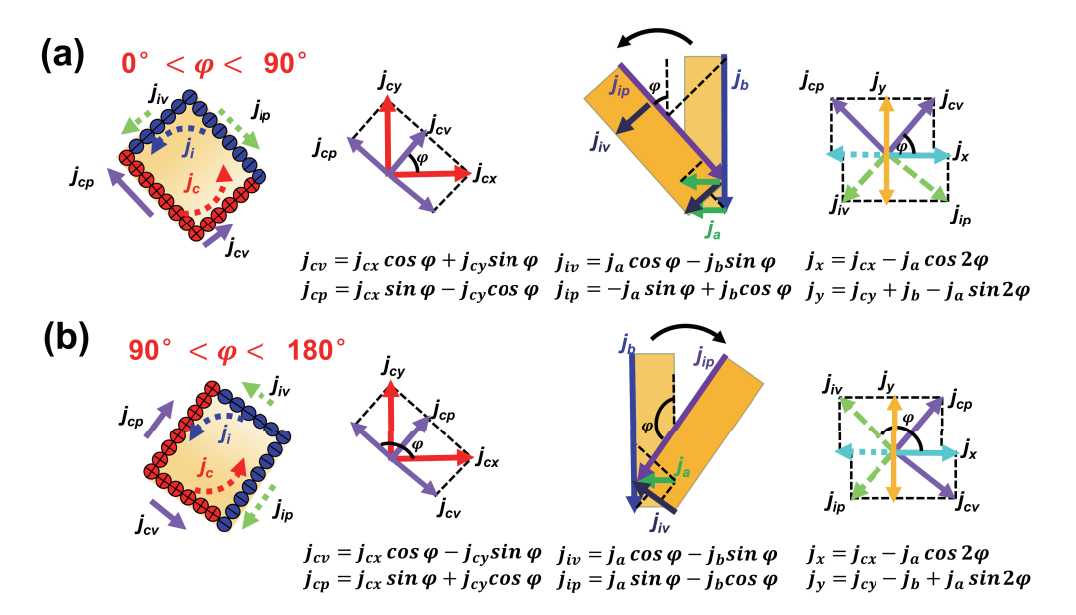


Figure B1 The decomposition of currents in the stripe. (a) Current distribution in samples when rotating to $\varphi(0^{\circ} < \varphi < 90^{\circ})$. (b) Current distribution in samples when rotating to $\varphi(90^{\circ} < \varphi < 180^{\circ})$.

Appendix C More details of the samples and the process of pattern fabrication

The fabrication of patterns was based on standard photolithography, etching and e-beam evaporation. The morphologies of patterns are observed by optical microscopy, as shown in Fig. C1.

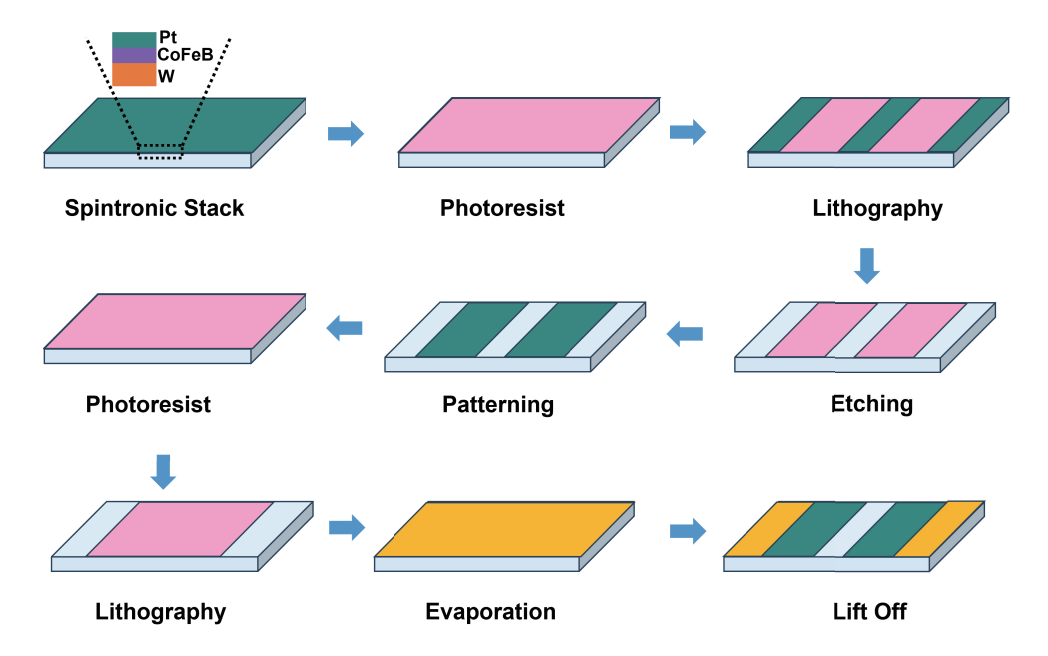


Figure C1 The decomposition of currents in the stripe. (a) Current distribution in samples when rotating to $\varphi(0^{\circ} < \varphi < 90^{\circ})$. (b) Current distribution in samples when rotating to $\varphi(90^{\circ} < \varphi < 180^{\circ})$.

Appendix D The control of inclination angle of elliptical polarization

Elliptical polarization can be regarded as consisting of two mutually orthogonal electric field components with a fixed phase difference. Here, the electric field component in the x-direction is donated as E_x , and the electric field component in the y-direction is donated as E_y . The general equation for an elliptically polarized wave can be written as:

$$E_x = E_{0x} cos \omega t,$$
 (D1)

$$E_y = E_{0y}cos(\omega t + \delta), \tag{D2}$$

where E_{0x} and E_{0x} are the amplitudes of the electric field components in the x and y directions, ω is the angular frequency, t is the time, δ is the phase difference between the two components.

After eliminating time t, we obtain:

$$(E_x/E_{0x})^2 + (E_y/E_{0y})^2 - 2(E_x/E_{0x})(E_y/E_{0y})\cos\delta = \sin 2\delta,$$
 (D3)

The ellipse depicted according to Eqs. (D3) is illustrated in the Fig. D1, with an inclination angle equal to the angle between the major axis of the ellipse and the reference coordinate axis.

The inclination angle α is equal to:

$$\alpha = \arctan(\mathbf{E}_{0x}\mathbf{E}_{0y}\cos\delta)/(\mathbf{E}_{0x}^2 - \mathbf{E}_{0y}^2), \tag{D4}$$

According to Eqs. (D4), the phase difference δ and the amplitude difference of E_{0x} and E_{0y} are key factors in controlling the inclination angle of the elliptical polarization states. Especially, when δ is 90°, the inclination angle is zero.

Based on spintronic-metasurface emitter we proposed, the amplitude and phase difference of the electric field components in the x and y directions are jointly influenced by the charge current j_{cx} and j_{cy} , the back flow j_a and j_b , and the azimuth angle, as shown in Eqs. (B9)- (B12).

According to the inverse spin Hall effect and the factors affecting the spin terahertz amplitude, the components of applied external magnetic field in the x and y direction M_x and M_y are the most critical factors controlling j_{cx} and j_{cy} . Moreover, the back flow is generated from the built-in electric field E_i inside the pattern, which can be expressed by

$$\alpha = \arctan(E_{\theta x} E_{\theta y} \cos \delta) / (E_{\theta x}^2 - E_{\theta y}^2), \tag{D5}$$

$$E_{\theta x} = \int_{\theta_2}^{arcsin(l/\sqrt{l^2 + w^2})) + \theta_1} 1/(4\pi\varepsilon_0) * \mathbf{Q_i}/w * sin\theta \ d\theta,$$
 (D6)

where l is the stripe length, w is the stripe width, ε_0 is the dielectric constant and $\mathbf{Q_i}$ represents linear charge density. Additionally, θ is the angle between d $\mathbf{E_i}$ formed by a pair of heterologous charges and the long edge, and $\theta_1(\theta_2)$ is the angle between d $\mathbf{E_i}$ and upper (lower) edge, respectively. It is evident that the aspect ratio plays a significant role in $\mathbf{j_a}$ and $\mathbf{j_b}$.

During the rotating process, the back flow and charges distribution are deeply affected by the azimuth angle, so each current can be affected by corresponding azimuth angles.

Therefore, the control of inclination angle can be achieved by adjusting the external magnetic field strength and distribution, fabricating stripe arrays with varying aspect ratios, and rotating the azimuth angles. We obtained the variation curves of the inclination angle with respect to the aspect ratio, magnetic field, and azimuth angle in the experiment based on Eqs. (D5), as shown in the Fig.D1(b)-(d).

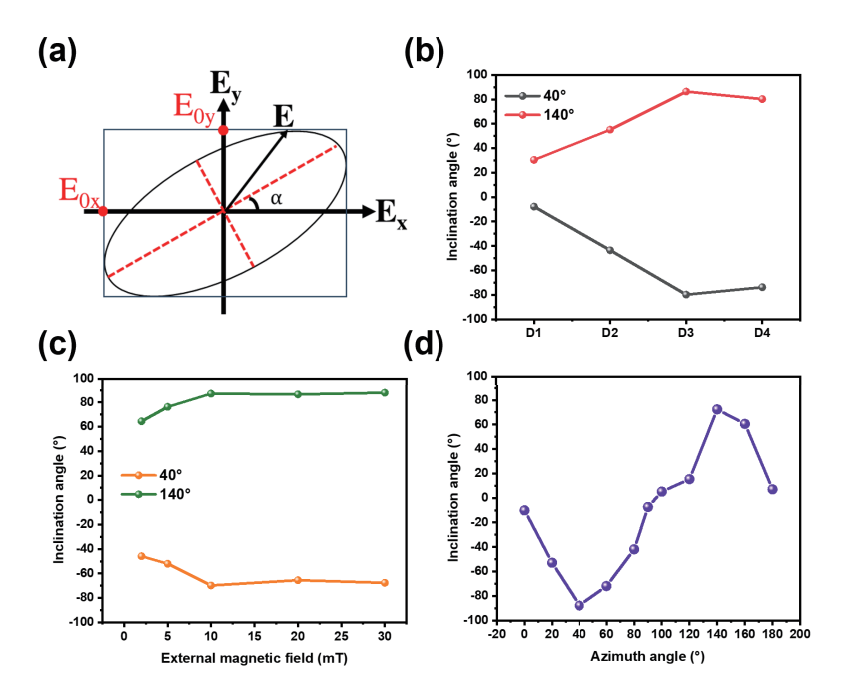


Figure D1 (a) The schematic diagram of elliptical polarization state. (b) The inclination angle varying with increasing aspect ratio under 30 mT nonuniform magnetic field at 40° and 140°. (c) The inclination angle of D4 varying with increasing magnetic field at 40° and 140°. (d) The inclination angle of D4 varying with rotating azimuth angles of D4 under 30 mT nonuniform magnetic field.